Int. J. Solids Structures Vol. 25, No. 9, pp. 999–1021, 1989
Printed in Great Britain.

0020–7683/89 $3.00 + .00

DEVELOPMENT OF A BOUNDARY ELEMENT METHOD FOR TIME-DEPENDENT PLANAR THERMOELASTICITY

G. F. DARGUSH and P. K. BANERJEE
Department of Civil Engineering, State University of New York at Buffalo, Buffalo, NY 14260, U.S.A.

(*Received* 18 *August* 1988)

Abstract—A new boundary element method is developed for two-dimensional quasistatic thermoelasticity. This time domain formulation involves only surface quantities. Consequently, volume discretization is completely eliminated and the method becomes a viable alternative to the usual finite element approaches. After presenting a brief overview of the governing equations, boundary integral equations for coupled quasistatic thermoelasticity are derived by starting with existing fundamental solutions along with an appropriate reciprocal theorem. Details of a general purpose numerical implementation are then discussed. Next, boundary element methods for the two more practical theories, uncoupled quasistatic and steady-state thermoelasticity, are developed directly from limiting forms of the coupled formulation. Several numerical examples are provided to illustrate the validity and attractiveness of the boundary element approach for this entire class of problems.

INTRODUCTION

In recent years, the boundary element method (BEM) has been extended to the analysis of a wide range of engineering problems. For many of these applications, the BEM is shown to provide an attractive alternative to the more popular finite element method, particularly when the formulation can be written exclusively in terms of boundary quantities. BEM, then, permits a reduction in the dimensionality of the problem. Thus, in a two-dimensional boundary element analysis, discretization is only needed along the bounding curve.

The present effort addresses planar problems in coupled quasistatic thermoelasticity (CQT), and details, for the first time, a boundary-only time domain BEM formulation and implementation. The more familiar uncoupled theories are shown to be just special cases of the coupled theory, and are solved within the same framework. For the uncoupled quasistatic case, this again represents a new development, while under steady-state conditions the well-established formulation of Rizzo and Shippy (1979) is recovered. Since considerable attention has focused on the thermoelastic problem, a brief review of the relevant BEM literature follows. Some references relating to poroelasticity are cited as well, because in the fully coupled case the governing differential equations for both theories have an identical form.

The early BEM work, carried out by Rizzo and Shippy (1977) and Cruse *et al.* (1977), pertained to steady-state thermoelasticity. The approach consisted of an initial phase in which a boundary element analysis of steady-state heat conduction was employed to determine the surface temperature and flux distribution. In the second phase, the resulting temperatures were applied as body forces in an elastostatic BEM to obtain deformation and stress. General properties of the steady-state temperature field were exploited to reduce the thermal body force volume integral to surface integrals involving the known boundary temperatures and flux. Thus, the entire two step process required only surface discretization.

In the quasistatic realm, Banerjee and Butterfield (1981) presented a staggered procedure for solving the coupled equations. The algorithm requires the solutions of the transient pore fluid (or heat) flow equation followed by an elastic analysis including body forces at each time step. Unfortunately, this is not a boundary-only formulation, and complete volume discretization is required. Cheng and Liggett (1984), on the other hand, investigated two-dimensional poroelasticity via a formulation in the Laplace transform

domain. While this is a boundary-only approach, the procedure is not, in general, satisfactory. The transform domain formulation is sensitive to the selection of values of the transform parameter, requires a numerical inversion of the transform, and is limited to strictly linear problems.

Returning to thermoelasticity, Tanaka and Tanaka (1981) presented a reciprocal theorem and the corresponding boundary element formulation for the time-domain coupled problem. However, kernel functions are not discussed and no numerical results are included. In fact, more recently, Tanaka *et al.* (1984) choose instead to implement the volume-based thermal body force approach of Banerjee and Butterfield. In a series of papers, Sládek and Sládek (1983, 1984a,b) presented a collection of fundamental solutions, in both Laplace transform and time domains, under the classifications of coupled, uncoupled, transient, and quasistatic thermoelasticity. Boundary integral equations were also included although in several instances these were written inappropriately in terms of displacement and traction rates. Kernel singularities were not discussed and a numerical implementation was not attempted. More recently, Chaudouet (1987) again resorts to the volume-based approach, while Masinda (1984) and Sharp and Crouch (1986) have directed efforts toward converting the thermal body force volume integral into a surface integral. Masinda, working in three dimensions, presents some formulations, but stops short before attempting an implementation. On the other hand, Sharp and Crouch develop an approach for two-dimensional quasistatic thermoelasticity using time-dependent Green's functions. However, the authors then introduce volume integrals in their time marching algorithm. This, unfortunately, undermines most of the advantages of the BEM.

In the following, boundary element formulations are developed for coupled quasistatic thermoelasticity (CQT), uncoupled quasistatic thermoelasticity (UQT), and steady-state thermoelasticity (SST). All three involve only boundary quantities, and, thus, discretization of the interior of the body is not required. These formulations have been implemented in GP-BEST, a large-scale boundary element computer program. As a result, quite general thermoelastic problems with arbitrary multi-region geometry and time-dependent boundary conditions can be solved. Details of the implementation are presented, as are several numerical examples to demonstrate the validity of the method.

COUPLED QUASISTATIC THEORY

Governing equations

Since a complete derivation of the thermoelastic theory can be found in the textbooks by Boley and Weiner (1960) and Nowacki (1986), only a few of the key assumptions will be mentioned before presenting the governing differential equations under plane strain conditions. In particular, the classical theory assumes infinitesimal deformations and linear isotropic materials. Thus, the linearized strain–displacement relationship

$$\varepsilon_{ij} = \tfrac{1}{2}(u_{i,j} + u_{j,i}) \tag{1}$$

is employed, along with constitutive laws of the form

$$\sigma_{ij} = \delta_{ij}\lambda\varepsilon_{kk} + 2\mu\varepsilon_{ij} - \delta_{ij}(3\lambda + 2\mu)\alpha(\theta - \theta_0) \tag{2}$$

$$q_i = -k\theta_{,i} \tag{3}$$

where

u_i	displacement vector
ε_{ij}	strain tensor
σ_{ij}	stress tensor
θ	present temperature
θ_0	temperature of a zero stress reference state
q_i	heat flux vector
λ, μ	Lame's isothermal elastic constants

α coefficient of thermal expansion
k thermal conductivity
δ_{ij} Kronecker's delta.

Then, application of the laws of conservation of momentum and energy lead, in the absence of inertia, to the following set of equations for plane strain:

$$(\lambda+\mu)u_{j,ij}+\mu u_{i,jj}-(3\lambda+2\mu)\alpha\theta_{,i}+f_i=0 \tag{4a}$$

$$k\theta_{,jj}-\rho c_\varepsilon\dot{\theta}-(3\lambda+2\mu)\alpha\theta_0\dot{u}_{j,j}+\psi=0, \tag{4b}$$

in which ρ is the mass density, c_ε is the specific heat at constant deformation, while f_i and ψ are the body forces and sources, respectively, and dots represent differentiation with respect to time. The theory portrayed by (4) is formally named Coupled Quasistatic Thermoelasticity (CQT). Notice, in particular, the appearance of displacement and temperature in both equations. Thus, in CQT not only do changes in temperature cause deformation, but also deformation produces temperature variations. In general, the set of equations (4) must be solved simultaneously. However, from an engineering viewpoint, it has been determined by a number of researchers (e.g. Boley and Weiner, 1960; Day, 1982) that the term involving displacement in (4b) is negligible, thus uncoupling the momentum and energy balance equations. Dropping that term, equation (4b) can first be solved independently for the temperature field. Subsequently, displacements are determined from (4a) with the known temperature distribution. This is, in fact, the accepted procedure for thermal stress analysis. For now, the general, fully coupled theory governed by (4) will be retained.

To complete the formulation of a well-posed problem, boundary and initial conditions must, of course, be specified. Formally, the boundary condition for all points x on S can be written as

$$u_i = U_i(X,t) \tag{5a}$$

or

$$t_i = T_i(X,t) \tag{5b}$$

or

$$t_i = K(X,t)u_i \tag{5c}$$

and

$$\theta = \Theta(X,t) \tag{6a}$$

or

$$q = Q(X,t) \tag{6b}$$

or

$$q = H(X,t)[\Theta_{amb}(X,t)-\theta]. \tag{6c}$$

In addition, the initial conditions

$$u_i = U_i^0(Z) \tag{7a}$$

$$\theta = \Theta^0(Z) \tag{7b}$$

are required for all points Z, in V at time zero which in the present analysis has been assumed to be zero for simplicity. In the above, q is that heat flux normal to the surface S, and t_i is the traction vector defined by

$$t_i = \sigma_{ji} n_j. \tag{8}$$

Note that (5c) and (6c) represent the familiar spring and convection boundary conditions, respectively, in which

$K(X, t)$	spring stiffness
$H(X, t)$	film coefficient
$\Theta_{amb}(X, t)$	ambient fluid temperature.

The specification of (5), (6) and (7) along with (4) completely defines the CQT problem.

Fundamental solutions

An essential ingredient in the development of a boundary integral equation for plane strain CQT is the appropriate time-dependent fundamental solutions. These required Green's functions have been derived by Rice and Cleary (1976) and Rudnicki (1987) within the context of the analogous theory of poroelasticity. Results are provided below after translation into standard thermoelastic nomenclature.

First, consider the effect of unit step forces acting in the j-direction at the points (ξ_1, ξ_2, x_3) where the range on x_3 is from $-\infty$ to $+\infty$. Thus, the applied force is a line load. The response, at any point $(x_1, x_2, 0)$, is given by

$$u_i(X, t) = \frac{1}{8\pi} \frac{1}{\mu(1-\nu)} \left[\left(\frac{y_i y_j}{r^2} \right) \bar{g}_1(\eta) + (\delta_{ij}) \bar{g}_2(\eta) \right] e_j \tag{9a}$$

$$\theta(X, t) = \frac{r}{2\pi} \left(\frac{\beta}{k(\lambda + 2\mu)} \right) \left[\left(\frac{y_j}{r} \right) \bar{g}_3(\eta) \right] e_j \tag{9b}$$

where

$$\beta = (3\lambda + 2\mu)\alpha \tag{10}$$

$$y_i = x_i - \xi_i \tag{11a}$$

$$r^2 = y_i y_i \tag{11b}$$

$$c = \frac{k}{\rho c_e} \frac{(\lambda + 2\mu)}{\left(\lambda + \dfrac{\theta_0 \beta^2}{\rho c_e} + 2\mu \right)} \tag{11c}$$

$$\eta = \frac{r}{(ct)^{1/2}} \tag{11d}$$

$$\bar{g}_1(\eta) = 1 + c_1 \{1 - \bar{h}_1(\eta)\} \tag{12a}$$

$$\bar{g}_2(\eta) = -(3 - 4\nu) \ln r + c_1 \{\bar{h}_2(\eta)\} \tag{12b}$$

$$\bar{g}_3(\eta) = \frac{\bar{h}_1(\eta)}{4t} \tag{12c}$$

and

$$c_1 = \frac{(1-2\nu)}{\lambda_s + 2\mu} \frac{\theta_0 \beta^2}{\rho c_e} = \frac{\nu_s - \nu}{1 - \nu_s} \tag{13}$$

$$\bar{h}_1(\eta) = \frac{4}{\eta^2} (1 - e^{-\eta^2/4}) \tag{14a}$$

$$\bar{h}_2(\eta) = \frac{1}{2}\left[E_1\left(\frac{\eta^2}{4}\right) + \ln\left(\frac{r^2}{4}\right) + \bar{h}_1\right]. \tag{14b}$$

The function E_1 is the exponential integral defined by

$$E_1(z) = \int_z^\infty \frac{e^{-x}}{x}\,dx. \tag{15}$$

Additionally, in (13) an isentropic Poisson ratio has been introduced for later use, where

$$\nu_s = \frac{\lambda_s}{2(\lambda_s + \mu)}. \tag{16}$$

Next, the continuous line heat source Green's function is presented. In this case, the resulting displacement and temperature fields are

$$u_i(X, t) = \frac{r}{4\pi}\left(\frac{\beta}{k(\lambda + 2\mu)}\right)\left[\left(\frac{y_i}{r}\right)\bar{g}_4(\eta)\right] \tag{17a}$$

$$\theta(X, t) = \frac{1}{2\pi}\left(\frac{1}{k}\right)[\bar{g}_5(\eta)] \tag{17b}$$

where

$$\bar{g}_4(\eta) = \frac{\bar{h}_1(\eta)}{2} + \frac{E_1\left(\frac{\eta^2}{4}\right)}{2} \tag{18a}$$

$$\bar{g}_5(\eta) = \frac{E_1\left(\frac{\eta^2}{4}\right)}{2}. \tag{18b}$$

It should be noted that, in the above, the evolution functions $\bar{g}_n(\eta)$ carry the solution from isentropic behavior at very short times to a final steady-state form at very long times.

Boundary integral formulation

A reciprocal theorem generally provides a convenient starting point for a direct boundary element formulation. For the coupled problem at hand, it appears that Ionescu-Cazimir (1964) was the first to explicitly state an appropriate reciprocal theorem, although certainly the groundwork was laid earlier by Biot (1959). In the context of Coupled Quasistatic Thermoelasticity, that theorem can be written, for a body of volume V and surface S with zero initial conditions, in the following time-domain form:

$$\int_S [\dot{t}_i^{(1)} * u_i^{(2)} + q^{(1)} * \theta^{(2)} - \dot{u}_i^{(1)} * t_i^{(2)} - \theta^{(1)} * q^{(2)}]\,dS$$

$$+ \int_V [\dot{f}_i^{(1)} * u_i^{(2)} + \psi^{(1)} * \theta^{(2)} - \dot{u}_i^{(1)} * f_i^{(2)} - \theta^{(1)} * \psi^{(2)}]\,dV = 0. \tag{19}$$

The superscripts $^{(1)}$ and $^{(2)}$ denote any two independent states existing in the body defined by $[\dot{u}_i^{(1)}, \dot{t}_i^{(1)}, \theta^{(1)}, q^{(1)}, \dot{f}_i^{(1)}, \psi^{(1)}]$ and $[u_i^{(2)}, t_i^{(2)}, \theta^{(2)}, q^{(2)}, f_i^{(2)}, \psi^{(2)}]$, respectively. The symbol $*$ indicates a Riemann convolution integral, where, for example

$$q^{(1)} * \theta^{(2)} = \int_0^t q^{(1)}(X, t-\tau)\theta^{(2)}(X, \tau)\, d\tau = \int_0^t q^{(1)}(X, \tau)\theta^{(2)}(X, t-\tau)\, d\tau. \tag{20}$$

It should be mentioned that the form of (19) above will lead to a boundary element formulation with displacement, traction, temperature and flux as primary quantities. Other researchers, notably Predeleanu (1981) and Sládek and Sládek (1984b), have written equally valid reciprocal statements that, unfortunately, lead to a much less desirable set of primary variables including, for example, displacement and traction rates.

Let one of the states above, say state (2), be the, as yet, unknown solution to a given boundary value problem defined by eqns (4)–(7). Then the remaining state may be chosen arbitrarily. However, by initially selecting for state (1), the infinite region response to a unit step continuous line force in the j-direction acting at ξ within V and beginning at time zero, the volume integrals in the reciprocal theorem can be made to vanish. That is, in equation (19), at any point Z in V, let the applied forces and sources equal

$$f_i^{(1)}(Z, t) = \delta(Z-\xi)H(t)\delta_{ij}e_j \tag{21a}$$

$$\psi^{(1)}(Z, t) = 0, \tag{21b}$$

and represent the response by

$$u_i^{(1)}(X, t) = G_{ij}(X-\xi, t)e_j \tag{21c}$$

$$\theta^{(1)}(X, t) = \dot{G}_{\theta j}(X-\xi, t)e_j \tag{21d}$$

$$t_i^{(1)}(X, t) = F_{ij}(X-\xi, t)e_j \tag{21e}$$

$$q^{(1)}(X, t) = \dot{F}_{\theta j}(X-\xi, t)e_j. \tag{21f}$$

In this notation, the subscript θ in (21d) and (21f) does not vary, but instead takes the value three for two-dimensional problems. Obviously, equations (21c) and (21d) are the same fundamental solutions that were presented in the previous sections, but now with a different nomenclature. On the other hand, the functions $F_{ij}(X-\xi, t)$ and $F_{\theta j}(X-\xi, t)$ can be obtained directly from G_{ij} and $G_{\theta j}$ through constitutive relationships. The superposed dots in (21d) and (21f) represent time derivatives which have been introduced for notational convenience. Ultimately, only the kernel functions G_{ij}, $G_{\theta j}$, F_{ij} and $F_{\theta j}$ will be required in explicit form.

Next for simplicity, assume that no body forces or heat sources exist in the actual boundary value problem. Then, the reciprocal relation, equation (19), can be rewritten

$$\int_S [\dot{F}_{ij}(X-\xi, t)e_j * u_i^{(2)}(X, t) + \dot{F}_{\theta j}(X-\xi, t)e_j * \theta^{(2)}(X, t) - \dot{G}_{ij}(X-\xi, t)e_j * t_i^{(2)}(X, t) - \dot{G}_{\theta j}(X-\xi, t)e_j * q^{(2)}(X, t)]\, dS(X) + \int_V [\delta(Z-\xi)\delta(t)\delta_{ij}e_j * u_i^{(2)}(Z, t)]\, dV(Z) = 0. \tag{22}$$

After some simplification, this becomes

$$\delta_{ij}u_i(\xi, t) = \int_S [\dot{G}_{ij}(X-\xi, t) * t_i(X, t) + \dot{G}_{\theta j}(X-\xi, t) * q(X, t) - \dot{F}_{ij}(X-\xi, t) * u_i(X, t) - \dot{F}_{\theta j}(X-\xi, t-\tau) * \theta(X, t)]\, dS(X), \tag{23}$$

in which the superscript (2) has now been dropped.

Equation (23) is an integral equation for interior displacement that involves only boundary quantities. Therefore, volume integration has, indeed, been eliminated through the use of an infinite space Green's function.

Evidently, equation (23) is the desired expression for the displacement vector at any interior point; however, a similar relationship is also desired for interior temperature. To that end, return to the reciprocal theorem (19) and select, instead, for state (1) the infinite space response to a unit pulse, continuous line heat source, acting at time zero and at point ξ within V. That is, let

$$f_i^{(1)}(Z,t) = 0 \tag{24a}$$

$$\psi^{(1)}(Z,t) = \delta(Z-\xi)\delta(t) \tag{24b}$$

and consequently,

$$u_i^{(1)}(X,t) = G_{i\theta}(X-\xi,t) \tag{24c}$$

$$\theta^{(1)}(X,t) = \dot{G}_{\theta\theta}(X-\xi,t) \tag{24d}$$

$$t_i^{(1)}(X,t) = F_{i\theta}(X-\xi,t) \tag{24e}$$

$$q^{(1)}(X,t) = \dot{F}_{\theta\theta}(X-\xi,t). \tag{24f}$$

Since this is the solution due to a unit pulse, the functions $G_{i\theta}$ and $\dot{G}_{\theta\theta}$ are the time derivatives of the unit step Green's functions presented previously. In the end, it will be the kernel functions $G_{i\theta}$, $G_{\theta\theta}$, $F_{i\theta}$ and $F_{\theta\theta}$ that will be of primary importance, rather than their time derivatives.

Now, again, state (2) is chosen to be the actual problem, in which body forces and heat sources are absent. Thus, the reciprocal theorem reduces finally to the form

$$\theta(\xi,t) = \int_S [G_{i\theta}(X-\xi,t) * t_i(X,t) + \dot{G}_{\theta\theta}(X-\xi,t) * q(X,t) - \dot{F}_{i\theta}(X-\xi,t) * u_i(X,t) - \dot{F}_{\theta\theta}(X-\xi,t) * (X,t)]\, dS(X). \tag{25}$$

This, of course, is the desired statement for interior temperatures in terms of boundary quantities.

Equations (23) and (25) can now be combined and rewritten in a more convenient matrix notation as

$$\begin{Bmatrix} u_j(\xi,t) \\ \theta(\xi,t) \end{Bmatrix} = \int_S \left(\begin{bmatrix} \dot{G}_{ij} & \dot{G}_{i\theta} \\ \dot{G}_{\theta j} & \dot{G}_{\theta\theta} \end{bmatrix}^T * \begin{Bmatrix} t_i(X,t) \\ q(X,t) \end{Bmatrix} - \begin{bmatrix} \dot{F}_{ij} & \dot{F}_{i\theta} \\ \dot{F}_{\theta j} & \dot{F}_{\theta\theta} \end{bmatrix}^T * \begin{Bmatrix} u_i(X,t) \\ \theta(X,t) \end{Bmatrix} \right) dS(X). \tag{26}$$

However, this can even be further compacted by generalizing the displacement and traction vectors to include temperature and flux, respectively, as an additional component. Thus, in two dimensions,

$$u_\alpha = \{u_1 \quad u_2 \quad \theta\}^T \tag{27a}$$

$$t_\alpha = \{t_1 \quad t_2 \quad q\}^T, \tag{27b}$$

where the Greek index α, and subsequently β, varies from one to three. Then (26) becomes simply

$$u_\alpha(\xi,t) = \int_S [\dot{G}_{\beta\alpha} * t_\beta(X,t) - \dot{F}_{\beta\alpha} * u_\beta(X,t)]\, dS(X). \tag{28}$$

Equation (28) can be viewed as a generalized Somigliana's identity for coupled quasistatic thermoelasticity, and, as such, is an exact statement for the interior displacements and

temperatures at any point ξ within V at any time t. However, to determine those interior quantities, the entire history of boundary values of u_α and t_α must be known. Unfortunately, in a well-posed boundary value problem only half of that information is given at each instant of time. In order to obtain the missing information, and in essence, solve the problem the point ξ must be moved to the boundary.

The process of writing (28) for a point on the boundary is not without complications, due to the singular nature of the kernel functions as $X \to \xi$ and $\tau \to t$. Considerable care must be exercised in evaluating these singular integrals. As a result, a constant matrix $c_{\beta\alpha}(\xi)$ is introduced and terms associated with $F_{\beta\alpha}$ must be treated as Cauchy principal value integrals. The new matrix $c_{\beta\alpha}$ is a function only of the local geometry of the boundary at ξ, and reduces to $\delta_{\beta\alpha}/2$ along a smooth surface.

With that in mind, the boundary integral formulation for CQT can be written

$$c_{\beta\alpha}(\xi)u_\beta(\xi,t) = \int_S [\dot{G}_{\beta\alpha} * t_\beta(X,t) - \dot{F}_{\beta\alpha} * u_\beta(X,t)]\, dS(X). \tag{29}$$

In principle, at each instant of time progressing from time zero, this equation can be written at every point on the boundary. The collection of the resulting equations could then be solved simultaneously, producing exact values for all the unknown boundary quantities. In reality, of course, discretization is needed to limit this process to a finite number of equations and unknowns.

Numerical implementation

The boundary integral equation (29) is an exact statement. No approximations have been introduced other than those used to formulate the boundary value problem. However, in order to apply (29) for the solution of practical engineering problems, approximations are required in both time and space.

For the temporal discretization, the time interval from zero to t is divided into N equal increments of duration Δt. Within each time increment, the primary field variables, t_β and u_β, are assumed constant. As a result, these quantities can be brought outside of the time integral. Since the integrand remaining is known in explicit form from the fundamental solutions, the required temporal integration can be performed analytically, and written as

$$G_{\beta\alpha}^{N+1\ n}(X-\xi) = \int_{(n-1)\Delta t}^{n\Delta t} \dot{G}_{\beta\alpha}(X-\xi, t-\tau)\, d\tau. \tag{30}$$

Combining this, and similar expressions for the $\dot{F}_{\beta\alpha}$ integral, with (29) produces

$$c_{\beta\alpha}(\xi)u_\beta^N(\xi) = \sum_{n=1}^{N} \int_S [G_{\beta\alpha}^{N+1-n}(X-\xi)t_\beta^n(X) - F_{\beta\alpha}^{N+1-n}(X-\xi)u_\beta^n(X)]\, dS(X). \tag{31}$$

The explicit form of the kernel functions, present in (31) are detailed in the Appendix.

The singularities, inherent in these kernels, when the load point and field point coincide, are of considerable importance. Series expansions of terms present in the evolution functions can be used to deduce the level of singularities existing in the kernels. Table 1 summarizes the results for plane strain CQT.

Table 1. Kernel singularities for plane strain CQT

Term	Level of singularity	Term	Level of singularity
G_{rr}^1	$\ln r$	F_{rr}^1	$\frac{1}{r}$
$G_{r\theta}^1$	non-singular	$F_{r\theta}^1$	non-singular
$G_{\theta r}^1$	non-singular	$F_{\theta r}^1$	$\ln r$
$G_{\theta\theta}^1$	$\ln r$	$F_{\theta\theta}^1$	$\frac{1}{r}$

A number of observations should be emphasized. First, as would be expected, $F^1_{\alpha\beta}$ has a stronger level of singularity than does the corresponding $G^1_{\alpha\beta}$, since an additional derivative is involved in obtaining $F^1_{\alpha\beta}$ from $G^1_{\alpha\beta}$. Second, the coupling terms do not have as a high degree of singularity as do the corresponding non-coupling terms. For example, compare $G^1_{i\theta}$ and $G^1_{\theta j}$ to G^1_{ij}. Third, all of the kernel functions for the first time step could actually be rewritten as a sum of steady-state and transient components. That is,

$$G^1_{\alpha\beta} = {}^{ss}G_{\alpha\beta} + {}^{tr}G^1_{\alpha\beta}$$
$$F^1_{\alpha\beta} = {}^{ss}F_{\alpha\beta} + {}^{tr}F^1_{\alpha\beta}.$$

Then, the singularity is completely contained in the steady-state portion. Furthermore, the singularity in G^1_{ij} and F^1_{ij} is precisely equal to that for elastostatics, while the $G^1_{\theta\theta}$ and $F^1_{\theta\theta}$ singularities are identical to those for potential flow. This observation is critical in the numerical integration of the $F_{\alpha\beta}$ kernel to be discussed in the next subsection. However, from a physical standpoint, this means simply that, at any time t, the nearer one moves toward the load point, the closer the quasistatic response field corresponds with a steady-state field. Eventually, when the sampling and load points coincide, the quasistatic and steady-state responses are indistinguishable. As a final item, after careful examination of the Appendix, it is evident that the steady-state components in the kernels $G^n_{\alpha\beta}$ and $F^n_{\alpha\beta}$, with $n > 1$, vanish. In that case, all that remains is a transient portion that contains no singularities. Thus, all singularities reside in the ${}^{ss}G_{\alpha\beta}$ and ${}^{ss}F_{\alpha\beta}$ components of $G^1_{\alpha\beta}$ and $F^1_{\alpha\beta}$, respectively.

Next, spatial discretization is introduced in order to evaluate the surface integrals appearing in (31). In the present implementation, both linear and quadratic boundary elements are available for the description of the geometry, as well as the primary field variables. Once the discretization is defined, the nodal generalized displacements and tractions can be brought outside the surface integral. Then, the remaining shape function–kernel products are integrated numerically. Sophisticated, self-adaptive integration algorithms are employed to ensure accuracy and numerical efficiency (Banerjee *et al.*, 1986 ; Ahmad and Banerjee, 1988).

With the discretization of the boundary integral equation, in both time and space, complete, a system of algebraic equations can be developed to permit the approximate solution of the original quasistatic problem. This is accomplished by systematically writing the integral equations at each global boundary node. The ensuing nodal collocation process produces a global set of equations of the form

$$\sum_{n=1}^{N} ([G^{N+1-n}]\{t^n\} - [F^{N+1-n}]\{u^n\}) = \{0\}, \tag{32}$$

in which $\{t^n\}$ and $\{u^n\}$ are nodal quantities with the superscript referencing the time step index. It should be noted that during this collocation process, the indirect "rigid body" technique (Cruse, 1974 ; Banerjee *et al.*, 1986) is employed to determine the strongly singular diagonal block of $[F^1]$.

In a well-posed problem, at any time t, the set of global generalized nodal displacements and tractions will contain exactly $3P$ unknown components,where P is the total number of functional nodes. Then, as the final stage in the assembly process, equation (32) can be rearranged to form (Banerjee *et al.*, 1986) :

$$[A^1]\{x^N\} = [B^1]\{y^N\} - \sum_{n=1}^{N-1} ([G^{N+1-n}]\{t^n\} - [F^{N+1-n}]\{u^n\}) \tag{33}$$

in which $\{x^N\}$ and $\{y^N\}$ represent the unknown and known nodal components, respectively. In addition, the summation represents the effect of past events. Thus, all quantities on the right-hand side of (33) are known at time step N.

It should be emphasized that the entire boundary element method presented, in this section, has involved surface quantities exclusively. A complete solution to the well-posed linear quasistatic problem, with homogeneous properties, can be obtained in terms of the nodal boundary response vectors, without the need for any volume discretization.

In many practical situations, however, additional information, such as the temperature at interior locations or the stress at points on the boundary, is required. Once equation (33) is solved, at any time step, the complete set of primary nodal quantities, $\{u^N\}$ and $\{t^N\}$, is known. Subsequently, the response at points within the body can be calculated in a straightforward manner. For any point ξ in the interior, the generalized displacement can be determined from (29) with $c_{\beta\alpha} = \delta_{\beta\alpha}$. However, when ξ is on the boundary, the strong singularity in ${}^{ss}F_{\beta\alpha}$ prohibits accurate direct evaluation of the generalized displacement, and an alternate approach is required. The apparent dilemma is easily resolved by recalling that the variation of surface quantities is completely defined by the elemental shape functions. Thus, for boundary points, the desired relationship is simply

$$u_\alpha^N(\xi) = N_{\omega}(\zeta) u_{\alpha\omega}^N \tag{34}$$

where $N_{\omega}(\zeta)$ are the shape functions for the appropriate element and ζ are the intrinsic coordinates. Obviously, from (34), neither integration nor the explicit contribution of past events are needed to evaluate generalized boundary displacements.

Meanwhile, interior stresses can be evaluated from

$$\sigma_{ij}^N(\xi) = \sum_{n=1}^{N} \left\{ \sum_{m=1}^{M} \left[t_{\beta\omega}^n \int_{S_m} E_{\beta ij}^{N+1-n}(X(\zeta) - \xi) N_{\omega}(\zeta)\, \mathrm{d}S(X(\zeta)) - u_{\beta\omega}^n \int_{S_m} D_{\beta ij}^{N+1-n}(X(\zeta) - \xi) N_{\omega}(\zeta)\, \mathrm{d}S(X(\zeta)) \right] \right\} \tag{35}$$

in which

$$E_{\alpha ij}^n(X(\zeta) - \xi) = \frac{2\mu\nu}{1-2\nu} \delta_{ij} \frac{\partial G_{\alpha l}^n}{\partial \xi_l} + \mu \left(\frac{\partial G_{\alpha i}^n}{\partial \xi_j} + \frac{\partial G_{\alpha j}^n}{\partial \xi_i} \right) - \beta \delta_{ij} G_{\alpha\theta}^n \tag{36a}$$

$$D_{\alpha ij}^n(X(\zeta) - \xi) = \frac{2\mu\nu}{1-2\nu} \delta_{ij} \frac{\partial F_{\alpha l}^n}{\partial \xi_l} + \mu \left(\frac{\partial F_{\alpha i}^n}{\partial \xi_j} + \frac{\partial F_{\alpha j}^n}{\partial \xi_i} \right) - \beta \delta_{ij} F_{\alpha\theta}^n. \tag{36b}$$

These are detailed in the Appendix.

Since strong kernel singularities appear when (35) is written for boundary points, surface stress can, instead, be obtained from

$$n_j(\xi) \sigma_{ij}^N(\xi) = N_{\omega}(\zeta) t_{i\omega}^N \tag{37a}$$

$$\sigma_{ij}^N(\xi) - \frac{D_{ijkl}^e}{2} (u_{k,l}^N(\xi) + u_{l,k}^N(\xi)) = -\beta \delta_{ij} N_{\omega}(\zeta) u_{\theta\omega}^N \tag{37b}$$

$$\frac{\partial x_j}{\partial \zeta} u_{i,j}^N(\xi) = \frac{\partial N_{\omega}}{\partial \zeta} u_{i\omega}^N \tag{37c}$$

in which $u_{\theta\omega}^N$ is obviously the nodal temperatures, and

$$D_{ijkl}^e = \lambda \delta_{ij} \delta_{kl} + 2\mu \delta_{ik} \delta_{jl}.$$

Equations (37), which are an extension of the technique developed by Cruse and VanBuren (1971), form an independent set that can be solved numerically for $\sigma_{ij}^N(\xi)$ and $u_{i,j}^N(\xi)$ completely in terms of known nodal quantities $u_{\alpha\omega}^N$ and $t_{i\omega}^N$, without the need for kernel integration or convolution. Notice, however, that shape function derivatives appear in

(37c), thus constraining the representation of stress on the surface element to something less than full quadratic variation.

The entire coupled quasistatic formulation has been implemented directly in GP-BEST, a state-of-the-art, general purpose boundary element computer program. Consequently, many additional features are available for the analysis of complex engineering problems, including multi-region capability, symmetry options, and a high degree of flexibility for the specification of boundary conditions.

UNCOUPLED QUASISTATIC THERMOELASTICITY

A simplification of CQT recovers the more traditional thermoelastic theory by ignoring the coupling in the energy equation. As discussed in Boley and Weiner (1960), the effect of this coupling for typical engineering materials is negligible within a quasistatic framework. Consequently, the resulting theory, labeled uncoupled quasistatic thermoelasticity or UQT, has a wide range of applicability. In this case, the governing differential equations (4) reduce to

$$(\lambda+\mu)u_{j,ij}+\mu u_{i,jj}-(3\lambda+2\mu)\alpha\theta_{,i}+f_i=0 \tag{38a}$$

$$k\theta_{,jj}-\rho c_\varepsilon\dot{\theta}+\psi=0. \tag{38b}$$

The practical significance of this simplification is that the energy equation no longer involves the deformation field. Thus, the temperature and flux can be obtained from (38b) as an independent initial phase. Subsequently, the deformation response is determined by satisfying (38a).

The kernel functions for UQT can be developed directly by considering limiting forms of the CQT kernels. In particular, the G_{ij} components reduce to their elastostatic counterparts, since unit forces in an uncoupled thermoelastic body produce a strictly instantaneous, isothermal response. As a further consequence of the unit force behavior, the $G_{i\theta}$ terms vanish. The remaining components of G are unchangd in form. However, for UQT, the diffusivity, upon which the evolution functions are based, becomes independent of the elastic properties, and reduces to its classical definition under conditions of transient heat conduction. Thus,

$$c=\frac{k}{\rho c_\varepsilon}. \tag{39}$$

With the nature of the kernel functions for UQT in mind, the integral equations (31) can be rewritten as

$$c_{00}(\xi)u_0^N(\xi)=\sum_{n=1}^{N}\int_S\left[G_{00}^{N+1-n}(X-\xi)t_0^n(X)-F_{00}^{N+1-n}(X-\xi)u_0^n(X)\right]\mathrm{d}S(X) \tag{40a}$$

$$c_{ij}(\xi)u_i^N(\xi)=\int_S\left[G_{ij}^1(X-\xi)t_i^N(X)-F_{ij}^1(X-\xi)u_i^N(X)\right]\mathrm{d}S(X)$$

$$+\sum_{n=1}^{N}\int_S\left[G_{0j}^{N+1-n}(X-\xi)t_0^n(X)-F_{0j}^{N-1-n}(x-\xi)u_0^n(X)\right]\mathrm{d}S(X). \tag{40b}$$

While these appear to be a bit more cumbersome than (31), significant computational advantages are present for UQT. Notice, in particular, that (40a) does not involve displacements nor tractions, and therefore can be solved independently as a single degree of freedom problem. Additionally, from (40b) it is obvious that the surface integrals involving G_{ij} and F_{ij} do not require time convolutions. In fact, convolution is only needed for the

temperature and flux terms, and for time steps beyond the first, all these kernels are non-singular. The result is a highly efficient boundary element method for UQT which involves only surface quantities.

STEADY-STATE THERMOELASTICITY

The second simplification of the general theory involves the removal of the time-dependent nature of the problem. As a consequence, it is assumed that loads are applied slowly, and that all of the resulting diffusive processes have been completed. In other words, the thermoelastic body is presumed to have reached steady-state. The governing differential equations now become

$$(\lambda+\mu)u_{j,ij}+\mu u_{i,jj}-(3\lambda+2\mu)\alpha\theta_{,i}+f_i=0 \tag{41a}$$

$$k\theta_{,jj}+\psi=0. \tag{41b}$$

Obviously, this is again an uncoupled theory, since the energy equation does not involve the deformation of the body. It is also a very practically significant theory, since the response of many structures must be examined under long-time loading, as well as during transients.

The fundamental solutions associated with (41) are simply the limiting forms of the quasistatic solutions. For example, the response to a unit step force at ξ in the j-direction is

$$u_i(X)=\frac{1}{8\pi}\frac{1}{\mu(1-\nu)}\left[\left(\frac{y_i y_j}{r^2}\right)+(\delta_{ij})(3-4\nu)\ln r\right]c_j \tag{42a}$$

$$\theta(X)=0, \tag{42b}$$

while the response due to a unit step heat source at ξ can be written as

$$u_i(X)=\frac{r}{8\pi}\left(\frac{\beta}{k(\lambda+2\mu)}\right)\left[\left(\frac{y_i}{r}\right)(1-2\ln r)\right] \tag{43a}$$

$$\theta(X)=\frac{1}{2\pi}\left(\frac{1}{k}\right)[\ln r]. \tag{43b}$$

The corresponding kernel functions developed from these Green's functions are, of course, identical to those that were derived by Rizzo and Shippy (1979) by another method.

With time-dependency completely eliminated, there is no longer any need for convolution integrals. Consequently, the boundary integral equations can be compacted to the form

$$c_{im}(\xi)u_m(\xi)=\int_\Gamma [G_{im}(X-\xi)t_m(X)-F_{im}(X-\xi)u_m(X)]\,dS(X) \tag{44a}$$

$$c_{ij}(\xi)u_i(\xi)=\int_\Gamma [G_{xj}(X-\xi)t_x(X)-F_{xj}(X-\xi)u_x(X)]\,dS(X). \tag{44b}$$

Once again, the thermal problem (44a) can be solved as an independent step, prior to the thermal stress analysis governed by (44b).

Under steady-state conditions, a plane stress boundary element method can be developed from the above by making the usual modifications of the thermoelastic constants. Thus, a plane stress problem with material properties E, ν and α is identical to the plane strain problem involving $\bar{E}$, $\bar{\nu}$ and $\bar{\alpha}$, where

$$\bar{E} = \frac{E(1+2\nu)}{(1+\nu)^2} \tag{45a}$$

$$\bar{\nu} = \frac{\nu}{1+\nu} \tag{45b}$$

$$\bar{\alpha} = \frac{\alpha(1+\nu)}{1+2\nu}. \tag{45c}$$

In the quasistatic case, it is, in general, not possible to fulfill the plane stress conditions and, at the same time, exactly satisfy the governing equations of three-dimensional thermoelasticity [see Boley and Weiner (1960) for a discussion]. However, the transformations noted in (45) can still be used to approximate plane stress solutions for thin bodies, although some caution is warranted.

APPLICATIONS

All three formulations (CQT, UQT and SST) have been implemented in a general purpose BEM system (GP-BEST). Because of extremely weak coupling, CQT and UQT produce almost identical answers, therefore in the time-dependent examples presented below, only UQT results are presented.

Circular disc

As a first example, transient thermal stresses in a circular disc are investigated. The disc of radius "a" initially rests at zero uniform temperature. The top and bottom surfaces are thermally insulated, and all boundaries are completely free of mechanical constraint. Then, suddenly, at time zero, the temperature of the entire outer edge (i.e. $r = a$) is elevated to unity and, subsequently, maintained at that level.

A GP-BEST boundary element model of the disc with unit radius is shown in Fig. 1. Only four quadratic elements are employed, along with quarter symmetry. Ten interior points are also included strictly to monitor response. In addition, the following non-dimensionalized material properties are arbitrarily selected for the plane stress analysis :

$$E = 1.333 \quad \rho c_\varepsilon = 1.0$$
$$\nu = 0.333 \quad k = 1.0.$$
$$\alpha = 0.75$$

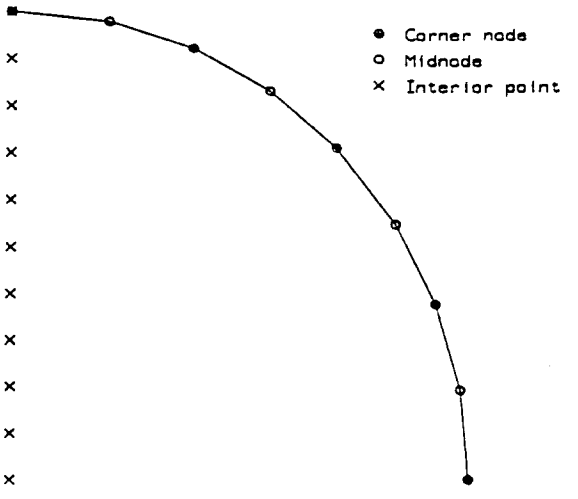

Fig. 1. Circular disc. Boundary element model.

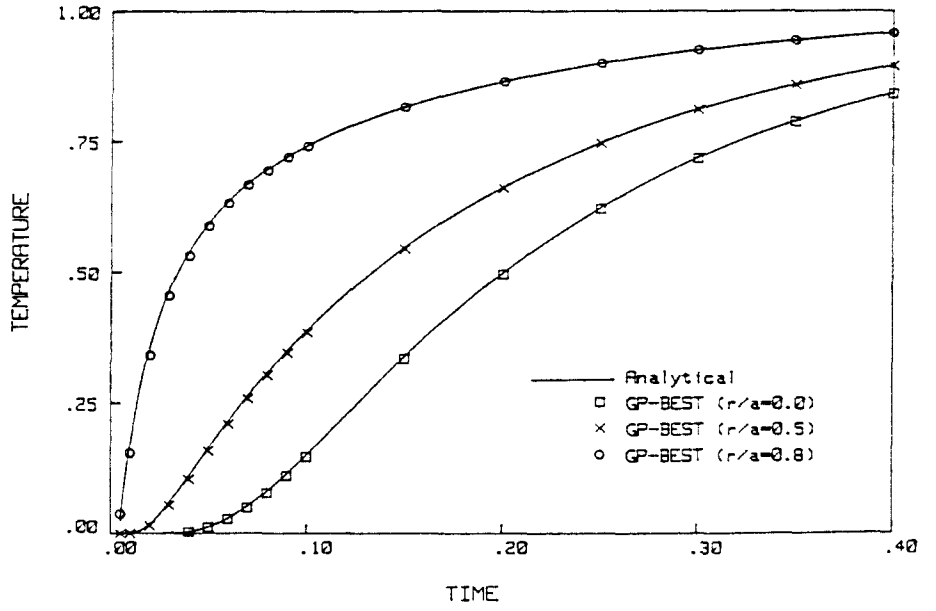

Fig. 2. Circular disc. GP-BEST results.

Results obtained under UQT for a time step of 0.005 are compared, in Figs. 2–4, to the analytical solution presented in Timoshenko and Goodier (1970). Notice that temperatures, as well as radial and tangential stresses are accurately determined via the boundary element analysis. In particular from Fig. 4, even the tangential stress on the outer edge is faithfully reproduced.

Bonded copper–brass bar

Consider next the thermal response of a composite formed by bonding a 16 in. long, 0.5 in. deep brass bar continuously to the top of a copper bar of the same dimensions. The assemblage, which is initially unstressed at zero temperature, is quickly heated by exposure to 200°F air on the top ($Y = 1.0$) and bottom ($Y = 0.0$) surfaces. A convection coefficient of 250 in.-lb./sec. in.^{2} °F is assumed for this process. The remaining surfaces are insulated. Meanwhile, all outer surfaces of the composite bar are considered traction free.

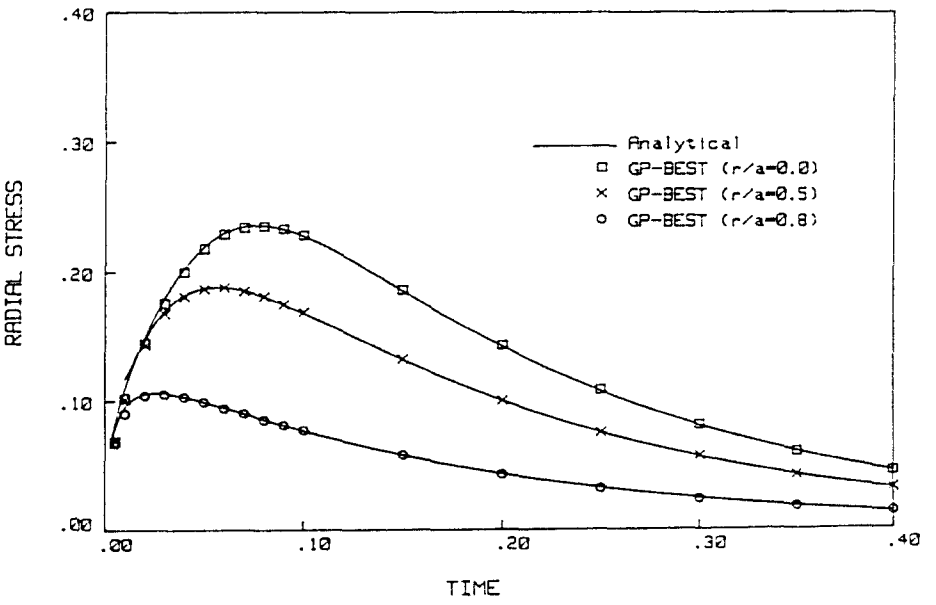

Fig. 3. Circular disc. GP-BEST results.

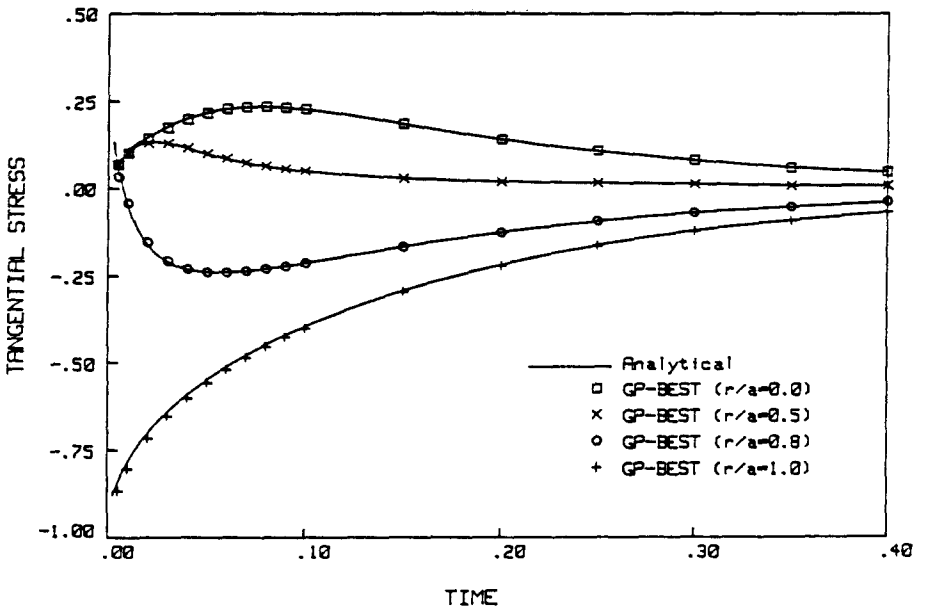

Fig. 4. Circular disc. GP-BEST results.

Figure 5 displays the boundary element model which necessarily includes separate generic modeling regions (GMRs) for the copper and brass components. Each GMR consists of 18 quadratic elements connecting 37 boundary nodes. Three interior points are also positioned inside each region along the $X = 0.0$ plane. Notice that symmetry is invoked on that $X = 0.0$ plane, so that only an 8 in. length of the bar is modeled. In addition to the boundary conditions mentioned above, the node at $X = 0.0$, $Y = 0.0$ is fixed in the Y-direction to prevent rigid body motion.

Standard room temperature properties are utilized for the two materials. Thus, for copper

$$E = 15.6 \times 10^6 \text{ psi} \qquad \rho c_\varepsilon = 278 \text{ in.-lb./in.}^3\,^\circ\text{F}$$
$$\nu = 0.355 \qquad k = 48 \text{ in.-lb/sec. in. }^\circ\text{F}$$
$$\alpha = 9.2 \times 10^{-6} \text{ in./in. }^\circ\text{F}$$

whereas for brass

$$E = 15.0 \times 10^6 \text{ psi} \qquad \rho c_\varepsilon = 274 \text{ in.-lb./in.}^3\,^\circ\text{F}$$
$$\nu = 0.364 \qquad k = 12 \text{ in.-lb./sec. in. }^\circ\text{F.}$$
$$\alpha = 11.8 \times 10^{-6} \text{ in./in. }^\circ\text{F}$$

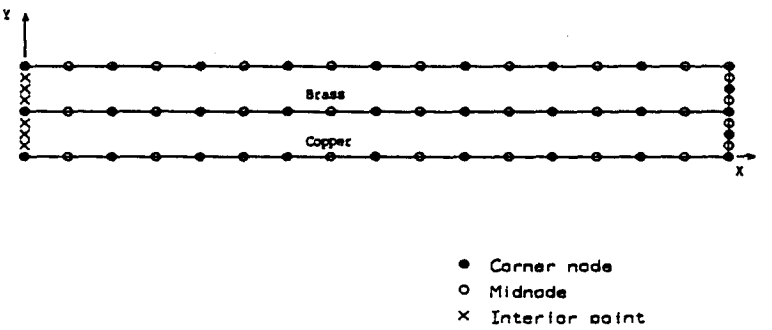

Fig. 5. Bonded copper–brass bar. Boundary element model.

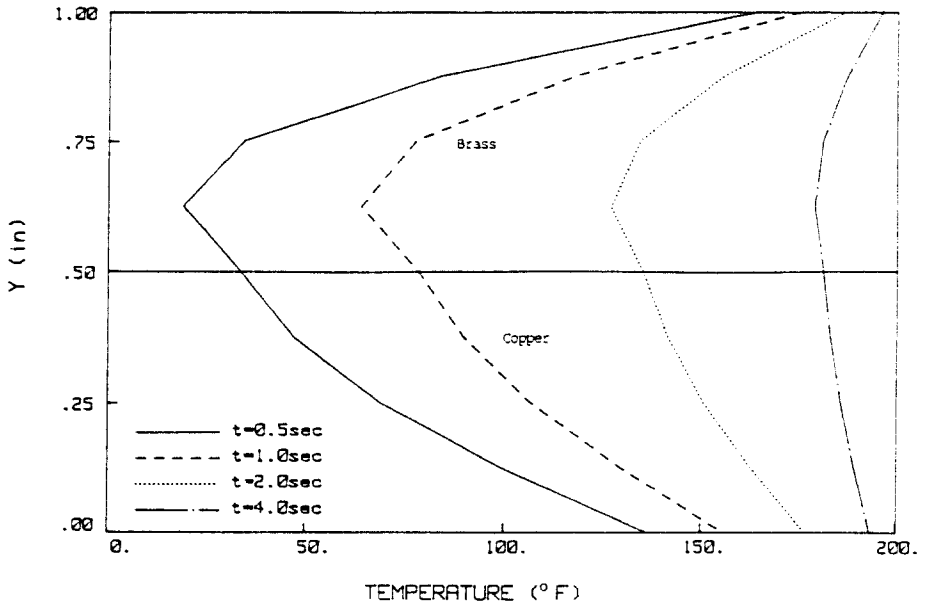

Fig. 6. Bonded copper–brass bar. GP-BEST results.

Based upon the material diffusivities and the characteristic element size, a time step of 0.050 s is selected for the GP-BEST analysis.

Naturally, due to differences in the thermal properties of the two materials, the temperature profile is not symmetric about the bonded interface. This is evident in the GP-BEST results displayed in Fig. 6, where temperatures are plotted vs depth at four distinct instants of time. Interestingly, although the copper component warms faster as a whole, at any given time the surface temperatures are always somewhat higher in the brass.

The transient thermal analysis, conducted under UQT conditions and summarized in Fig. 6, is completely independent of the thickness. Such is not the case for the displacement and stress response. Consequently, in the present analysis, both plane strain (i.e. very thick) and plane stress (i.e. very thin) approximations are examined. Figure 7 depicts the downward vertical deflection with time for a point ($X = 8.0$, $Y = 0.0$) at one end of the bar. This bending is the result of the non-symmetric temperature profile mentioned above, along with the mismatch in coefficients of thermal expansion. Longitudinal stresses, away

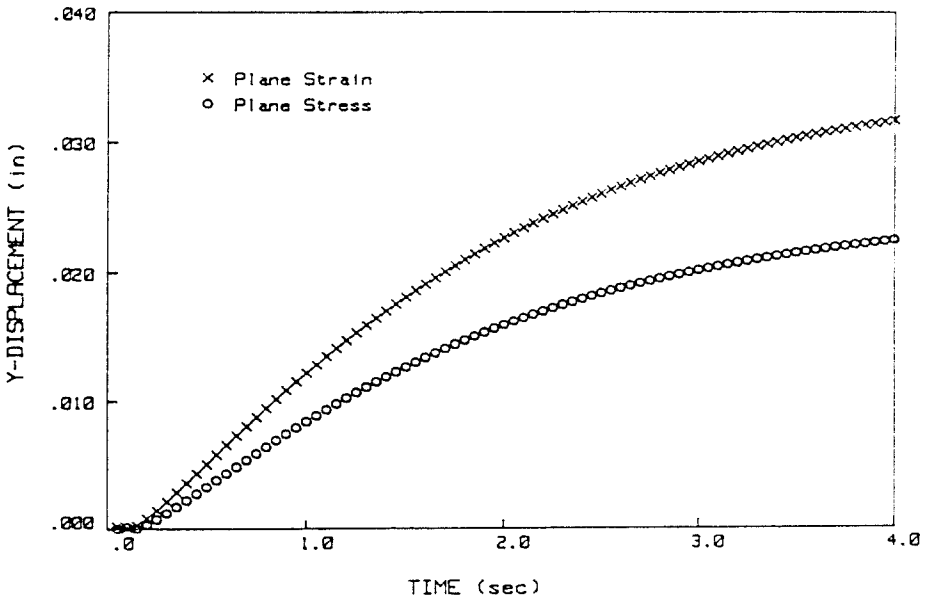

Fig. 7. Bonded copper–brass bar. GP-BEST results.

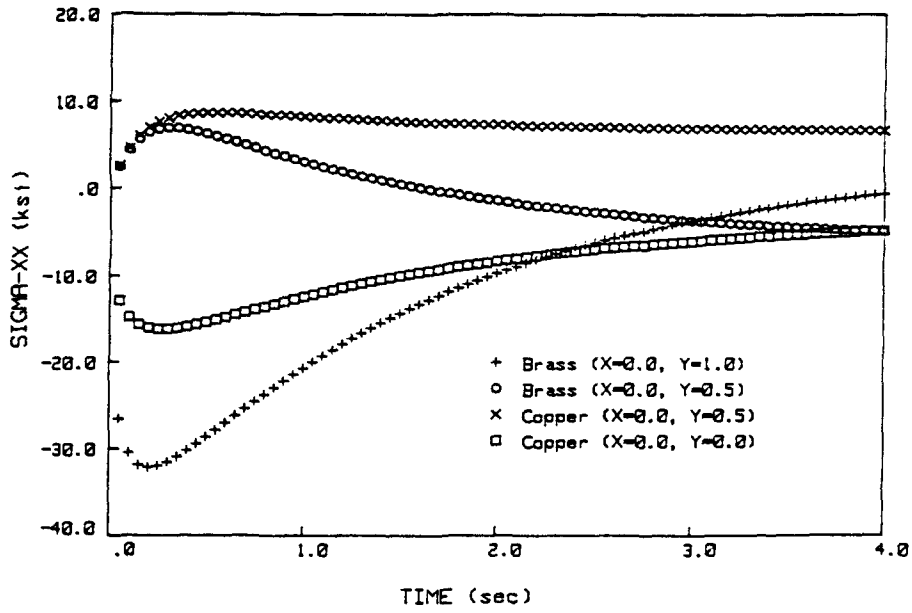

Fig. 8. Bonded copper–brass bar. Plane strain.

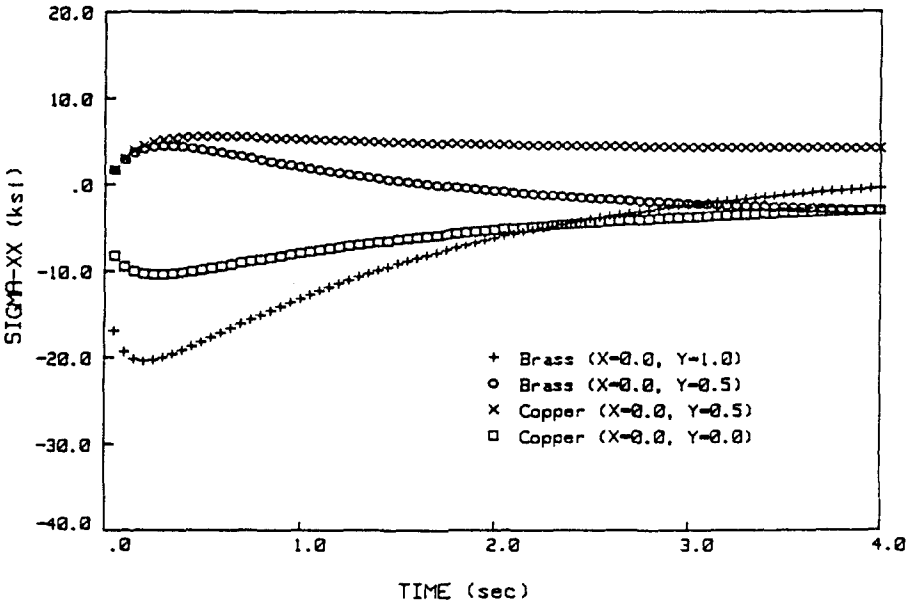

Fig. 9. Bonded copper–brass bar. Plane stress.

from the ends, are plotted in Figs 8 and 9 for plane strain and plane stress, respectively. In both cases, the transient thermal stresses are significantly higher than their steady-state counterparts. Of course, the steady-state solution can be obtained either by continuing the transient algorithm for a large number of time steps or by directly using the steady-state kernels. The latter approach produces the results presented in Table 2. Notice that the

Table 2. Steady-state results for a bonded copper–brass bar

	Plane strain	Plane stress
Tip deflection (in.)	0.035	0.025
Longitudinal stress (ksi)		
Brass ($X = 0.0$, $Y = 1.0$)	+3.1	+1.9
Brass ($X = 0.0$, $Y = 0.5$)	−6.3	−3.9
Copper ($X = 0.0$, $Y = 0.5$)	+6.4	+4.0
Copper ($X = 0.0$, $Y = 0.0$)	−3.2	−2.0

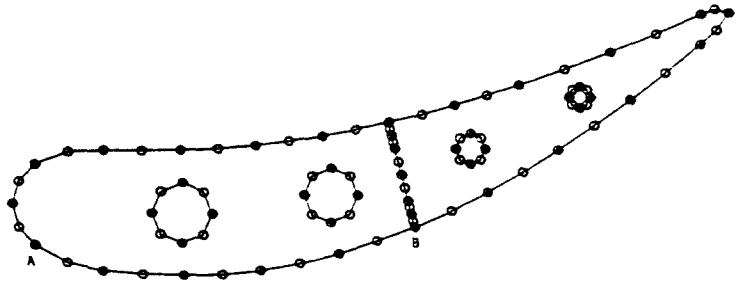

Fig. 10. Turbine blade. Boundary element model.

plane stress formulation, as would be expected, consistently provides lower magnitudes for deformation and stress for this thermally-driven problem.

Turbine blade

For the final application, the plane strain response of an internally cooled turbine blade is examined under startup thermal transients. The boundary element model of the blade is illustrated in Fig. 10. In this problem, the two GMR approach is chosen solely to enhance computational efficiency. This is accomplished by reducing the aspect ratio of individual GMRs and by creating a block banded system matrix. The leading (left-hand) GMR consists of 26 quadratic elements, while 24 elements are used to model the trailing (right-hand) region.

The blade is manufactured of stainless steel with the following thermomechanical properties:

$$E = 29.0 \times 10^6 \text{ psi} \qquad \rho c_\varepsilon = 368 \text{ in.-lb./in.}^3\,^\circ\text{F}$$

$$\nu = 0.30 \qquad k = 1.65 \text{ in.-lb./sec. in. }^\circ\text{F}.$$

$$\alpha = 9.6 \times 10^{-6} \text{ in./in. }^\circ\text{F}$$

During operation a hot gas flows outside the blade, while a relatively cool gas passes through the internal holes. The gas temperature transients are plotted in Fig. 11 for a typical startup. Convection film coefficients are specified as follows:

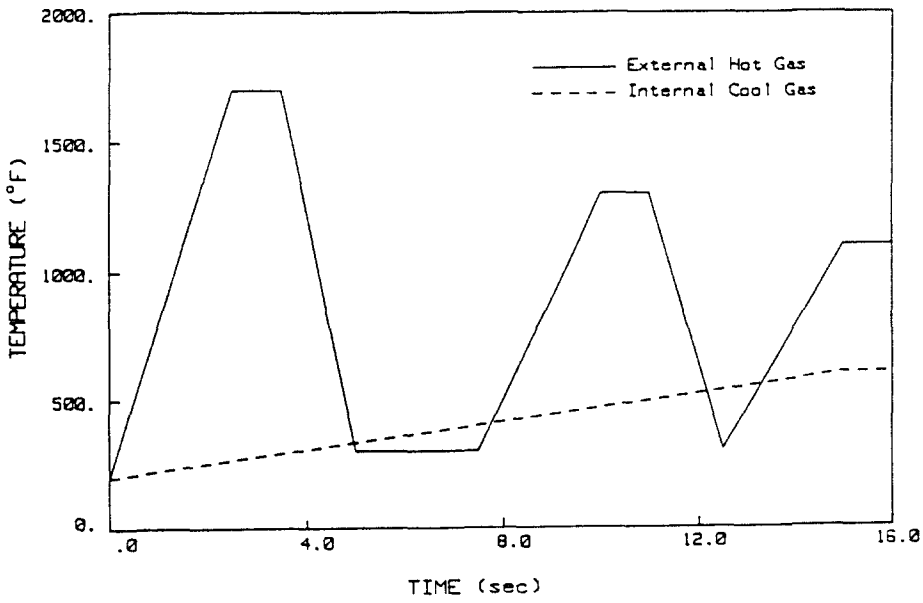

Fig. 11. Turbine blade. Startup transient.

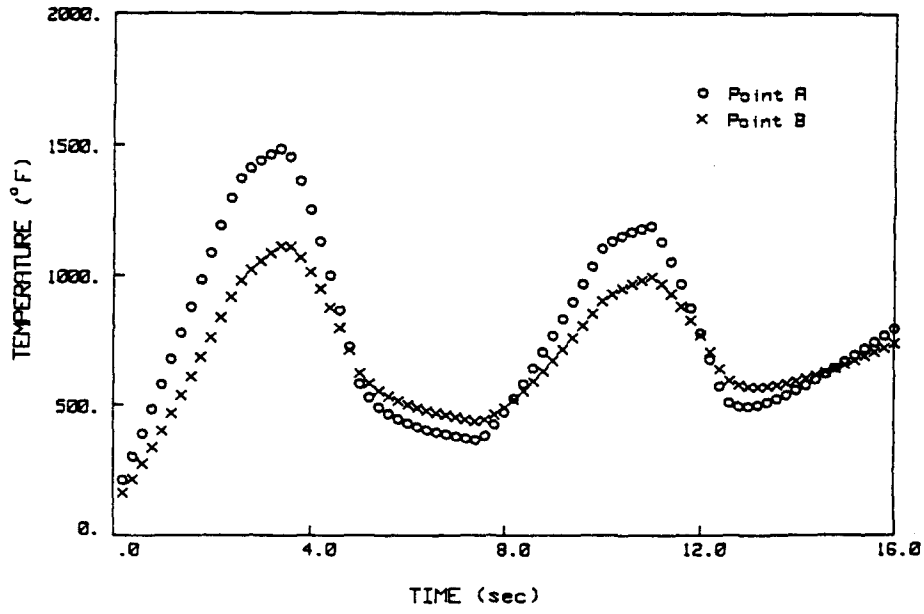

Fig. 12. Turbine blade. GP-BEST results.

Outer surface at leading edge	$h = 50$ in.-lb./sec. in.^{2} °F
Remainder of outer surface	$h = 20$ in.-lb./sec. in.^{2} °F
Inner cooling hole surfaces	$h = 10$ in.-lb./sec. in.^{2} °F.

A time step of 0.2 s is employed for the UQT GP-BEST analysis.

The response at two points A, on the leading edge and, B, at midspan are displayed in Figs 12 and 13. Notice that temperatures and stresses are consisently higher on the leading edge, reaching peak values of approximately 1500 °F and −60 ksi, respectively. Also, as is evident from Fig. 13, significant stress reversals occur during this startup. As a next step, these results from GP-BEST could be used as input for a fatigue analysis to assess the durability of the design. In that regard, it should be emphasized that the stresses presented for points A and B are surface stresses, calculated by satisfying the constitutive

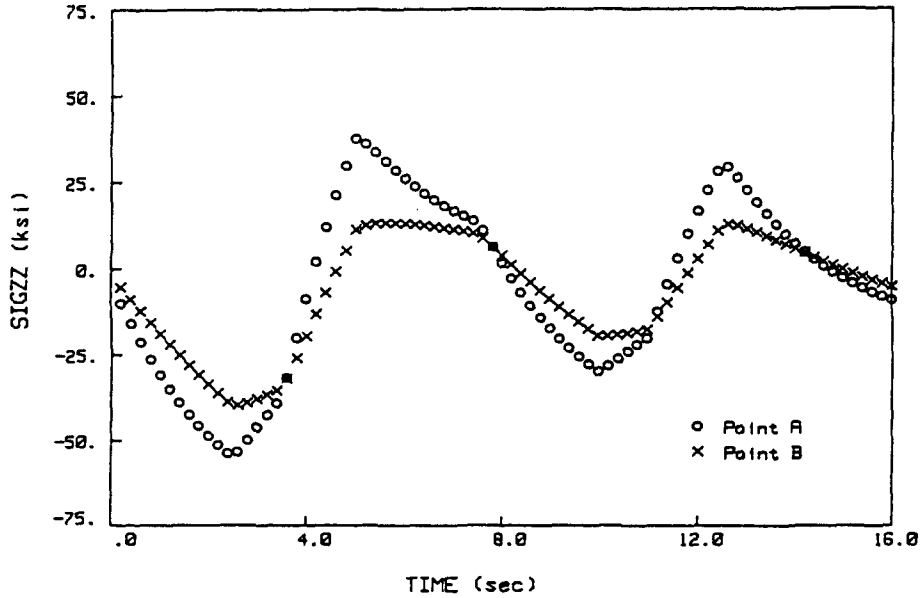

Fig. 13. Turbine blade. GP-BEST results.

laws, strain–displacement and equilibrium directly at the boundary point. This can be expected to produce much more accurate results than the standard practice utilized in finite element approaches of extrapolating interior Gauss point stress values to the boundary.

CONCLUSIONS

In the present work, the boundary element method is extended to transient problems of two-dimensional thermoelasticity. Integral formulations are first developed for coupled quasistatic thermoelasticity, and then specialized to the more practical theories of uncoupled quasistatic and steady-state thermoelasticity. The resulting steady-state formulation reduces to that given by Rizzo and Shippy (1979). However, the new time-domain quasistatic formulations also require only surface discretization, and consequently, are viable alternatives to finite element analysis for this class of problems. In addition, steep thermal gradients, which often occur near the surface, can be more readily captured, since with the boundary element approach there are no shape functions to constrain the solution in the direction normal to the surface. For example, the circular disc analysis indicates the level of accuracy that is obtainable with the present BEM.

All three thermoelastic formulations are implemented, for both plane strain and plane stress, in GP-BEST, a general purpose boundary element code. As a result, realistic thermoelastic engineering analysis can be performed. The three detailed examples highlight the validity of the formulations and some potential applications.

Acknowledgements—The work described in this paper was made possible by a grant from United Technologies Corporation. The authors are indebted to Drs R. B. Wilson and E. Todd of Pratt and Whitney for their support and encouragement.

REFERENCES

Ahmad, S. and Banerjee, P. K. (1988). Transient elastodynamic analysis of three-dimensional problems by BEM. *Int. J. Numer. Meth. Engng* **26**(8), 1560–1580.

Banerjee, P. K., Ahmad, S. and Manolis, G. D. (1986). Transient elastodynamic analysis of three-dimensional problems by boundary element method. *Earthquake Engng Structural Dyna.* **14**, 933–949.

Banerjee, P. K. and Butterfield, R. (1981). *Boundary Element Methods in Engineering Science*. McGraw-Hill, London.

Biot, M. A. (1959). New thermomechanical reciprocity relations with application to thermal stress analysis. *J. Aerospace Sci.* **26**(7), 401–408.

Boley, B. A. and Weiner, J. H. (1960). *Theory of Thermal Stresses*. John Wiley and Sons, New York.

Chaudouet, A. (1987). Three-dimensional transient thermoelastic analysis by the BIE method. *Int. J. Numer. Meth. Engng* **24**, 25–45.

Cheng, A. H.-D. and Liggett, J. A. (1984). Boundary integral equation method for linear porous-elasticity with applications to soil consolidation. *Int. J. Numer. Meth. Engng* **20**, 255–278.

Cruse, T. A. (1974). An improved boundary integral equation method for three-dimensional elastic stress analysis. *Comput. Struct.* **4**, 741–754.

Cruse, T. A. Snow, D. W. and Wilson, R. B. (1977). Numerical solutions in axisymmetric elasticity. *Comput. Struct.* **7**, 445–451.

Cruse, T. A. and VanBuren, W. (1971). Three-dimensional elastic stress analysis of a fracture specimen with an edge crack. *Int. J. Fract. Mech.* **7**, 1–16.

Day, W. A. (1982). Further justification of the uncoupled and quasi-static approximations in thermoelasticity. *Arch. Ratl Mech. Anal.* **79**(1), 387–396.

Ionescu-Cazimir, V. (1964). Problem of linear coupled thermoelasticity. Theorems on reciprocity for the dynamic problem of coupled thermoelasticity. I. *Bull. Acad. Polonaise Sci. Series Sci. Tech.* **12**(9), 473–488.

Masinda, J. (1984). Application of the boundary elements method to 3D problems of non-stationary thermoelasticity. *Engng Anal.* **1**, 66–69.

Nowacki, W. (1986). *Thermoelasticity*. Pergamon, Warsaw.

Predeleanu, M. (1981). Boundary integral method for porous media. In *Boundary Methods* (Edited by C. A. Brebbia), pp. 325–334. Springer, New York.

Rice, J. R. and Cleary, M. P. (1976). Some basic stress diffusion solutions for fluid-saturated elastic porous media and compressible constituents. *Rev. Geophys. Space Phys.* **14**(2), 227–241.

Rizzo, F. J. and Shippy, D. J. (1977). An advanced boundary integral equation method for three-dimensional thermoelasticity. *Int. J. Numer. Meth. Engng* **11**, 1753–1768.

Rizzo, F. J. and Shippy, D. J. (1979). The boundary element method in thermoelasticity. In *Developments in Boundary Element Methods—1* (Edited by P. K. Banerjee and R. Butterfield). Applied Science Publishers, London.

Rudnicki, J. W. (1987). Fluid mass sources and point forces in linear elastic diffusive solids. *Mech. Mater.* **5**, 383–393.

Sharp, S. and Crouch, S. L. (1986). Boundary integral methods for thermoelasticity problems. *J. Appl. Mech.* **53**, 298–302.
Sládek, V. and Sládek, J. (1983). Boundary integral equation method in thermoelasticity Part I: General analysis. *Appl. Math. Modelling* **7**, 241–253.
Sládek, V. and Sládek, J. (1984a). Boundary integral equation method in thermoelasticity Part III: Uncoupled thermoelasticity. *Appl. Math. Modelling* **8**, 413–418.
Sládek, V. and Sládek, J. (1984b). Boundary integral equation method in two-dimensional thermoelasticity. *Engng Anal.* **1**, 135–148.
Tanaka, M. and Tanaka, K. (1981). Boundary element approach to dynamic problems in coupled thermoelasticity—1. Integral equation formulation. *Solid Mech. Arch.* **6**, 467–491.
Tanaka, M., Togoh, H. and Kikuta, M. (1984). Boundary element method applied to 2-D thermoelastic problems in steady and non-steady states. *Engng Anal.* **1**, 13–19.
Timoshenko, S. P. and Goodier, J. N. (1970). *Theory of Elasticity*. McGraw-Hill, New York.

APPENDIX: COUPLED QUASISTATIC THERMOELASTIC KERNELS

Two-dimensional (plane strain) kernels are provided, based upon continuous source and force fundamental solutions. As a result, the following relationships must be used to determine the proper form of the functions required in the boundary element discretization. That is,

$$G^n_{\alpha\beta}(X-\xi) = G_{\alpha\beta}(X-\xi, n\Delta t) \qquad \text{for } n = 1$$
$$G^n_{\alpha\beta}(X-\xi) = G_{\alpha\beta}(X-\xi, n\Delta t) - G_{\alpha\beta}(X-\xi, (n-1)\Delta t) \qquad \text{for } n > 1,$$

with similar expressions holding for all the remaining kernels. In the specification of these kernels below, the arguments $(X-\xi, t)$ are assumed.

In two dimensions, the indices

i, j, k, l	vary from 1 to 2
α, β	vary from 1 to 3
θ	equals 2.

Additionally,

x_i coordinates of integration point

ξ_i coordinates of field point

$$y_i = x_i - \xi_i$$
$$r^2 = y_i y_i$$
$$\eta = \frac{r}{(ct)^{1/2}}$$
$$c_1 = \frac{(1-2\nu)}{\lambda_s + 2\mu}\frac{\theta_0\beta^2}{\rho c_s} = \frac{\nu_s - \nu}{1-\nu_s}$$
$$c = \frac{k}{\rho c_s}\frac{\lambda+2\mu}{\lambda_s+2\mu}.$$

For the displacement kernel,

$$G_{ij} = \frac{1}{8\pi}\frac{1}{\mu(1-\nu)}\left[\left(\frac{y_i y_j}{r^2}\right)\bar{g}_1(\eta) + (\delta_{ij})\bar{g}_2(\eta)\right]$$
$$G_{i\theta} = \frac{r}{2\pi}\left(\frac{\beta}{k(\lambda+2\mu)}\right)\left[\left(\frac{y_i}{r}\right)\bar{g}_3(\eta)\right]$$
$$G_{\theta j} = \frac{r}{2\pi}\left(\frac{\beta}{k(\lambda+2\mu)}\right)\left[\left(\frac{y_j}{r}\right)\bar{g}_4(\eta)\right]$$
$$G_{\theta\theta} = \frac{1}{2\pi}\left(\frac{1}{k}\right)[\bar{g}_5(\eta)]$$

whereas, for the traction kernel,

$$F_{ij} = \frac{1}{4\pi r}\frac{1}{(1-\nu)}\left[-\left(\frac{y_i y_j y_k n_k}{r^3}\right)\bar{f}_1(\eta) - \left(\frac{\delta_{ij}y_k n_k + y_i n_j}{r}\right)\bar{f}_2(\eta) + \left(\frac{y_j n_i}{r}\right)\bar{f}_3(\eta)\right]$$
$$F_{i\theta} = \frac{1}{\pi}\left(\frac{\mu\beta}{k(\lambda+2\mu)}\right)\left[\left(\frac{y_i y_k n_k}{r^2}\right)\bar{f}_4(\eta) + (n_i)\bar{f}_5(\eta)\right]$$

$$F_{ij} = \frac{1}{4\pi}\left(\frac{\beta}{\lambda+2\mu}\right)\left[\left(\frac{y_i y_k n_k}{r^2}\right)\bar{f}_6(\eta) - (n_j)\,\bar{f}_7(\eta)\right]$$

$$F_{i\theta} = \frac{1}{2\pi r}\left[\left(\frac{y_k n_k}{r}\right)\bar{f}_8(\eta)\right].$$

In the above,

$$E_1(z) = \int_z^\infty \frac{e^{-x}}{x}\,dx$$

$$\bar{h}_1(\eta) = \frac{4}{\eta^2}(1-e^{-\eta^2/4})$$

$$\bar{h}_2(\eta) = \frac{1}{2}\left[E_1\left(\frac{\eta^2}{4}\right) + \ln\left(\frac{r^2}{4}\right) + \bar{h}_1\right]$$

$$\bar{g}_1(\eta) = 1 + c_1\{1-\bar{h}_1(\eta)\}$$

$$\bar{g}_2(\eta) = -(3-4\nu)\ln r + c_1\{\bar{h}_2(\eta)\}$$

$$\bar{g}_3(\eta) = \frac{\bar{h}_1(\eta)}{4t}$$

$$\bar{g}_4(\eta) = \frac{\bar{h}_1(\eta)}{2} + \frac{E_1\left(\frac{\eta^2}{4}\right)}{2}$$

$$\bar{g}_5(\eta) = \frac{E_1\left(\frac{\eta^2}{4}\right)}{2}$$

$$\bar{f}_1(\eta) = 2 + 2c_1\{1+e^{-\eta^2/4} - 2\bar{h}_1(\eta)\}$$

$$\bar{f}_2(\eta) = (1-2\nu) - c_1\{1-\bar{h}_1(\eta)\}$$

$$\bar{f}_3(\eta) = (1-2\nu) - c_1\{1-2e^{-\eta^2/4} + \bar{h}_1(\eta)\}$$

$$\bar{f}_4(\eta) = \frac{e^{-\eta^2/4}}{2t} - \frac{\bar{h}_1(\eta)}{2t}$$

$$\bar{f}_5(\eta) = \frac{\bar{h}_1(\eta)}{4t} - \frac{e^{-\eta^2/4}}{2t}$$

$$\bar{f}_6(\eta) = \bar{h}_1(\eta)$$

$$\bar{f}_7(\eta) = \frac{\bar{h}_1(\eta)}{2} + \frac{E_1\left(\frac{\eta^2}{4}\right)}{2}$$

$$\bar{f}_8(\eta) = e^{-\eta^2/4}.$$

For the interior stress kernels,

$$E_{xij} = \frac{2\mu\nu}{1-2\nu}\delta_{ij}\frac{\partial G_{xl}}{\partial \xi_l} + \mu\left(\frac{\partial G_{xi}}{\partial \xi_j} + \frac{\partial G_{xj}}{\partial \xi_i}\right) - \beta\delta_{ij}G_{x0}$$

$$D_{xij} = \frac{2\mu\nu}{1-2\nu}\delta_{ij}\frac{\partial F_{xl}}{\partial \xi_l} + \mu\left(\frac{\partial F_{xi}}{\partial \xi_j} + \frac{\partial F_{xj}}{\partial \xi_i}\right) - \beta\delta_{ij}F_{x0}$$

where

$$\frac{\partial G_{ij}}{\partial \xi_k} = \frac{1}{8\pi r}\frac{1}{\mu(1-\nu)}\left[\left(\frac{2y_i y_j y_k}{r^3} - \frac{\delta_{jk}y_i}{r} - \frac{\delta_{ik}y_j}{r}\right)\bar{g}_1(\eta) + \left(\frac{2y_i y_j y_k}{r^3}\right)\{c_1(e^{-\eta^2/4} - \bar{h}_1)\} + \left(\frac{\delta_{ij}y_k}{r}\right)\{(3-4\nu) - c_1(1-\bar{h}_1)\}\right]$$

$$\frac{\partial G_{0j}}{\partial \xi_k} = \frac{1}{4\pi}\left(\frac{\beta}{k(\lambda+2\mu)}\right)\left[\left(\frac{y_j y_k}{r^2}\right)\{\bar{h}_1\} - (\delta_{jk})\left\{\frac{\bar{h}_1}{2} + \frac{E_1(\eta)}{2}\right\}\right]$$

$$\frac{\partial F_{ij}}{\partial \xi_k} = \frac{1}{4\pi r^2}\frac{1}{(1-\nu)}\left[-\left(\frac{4y_i y_j y_k y_l n_l}{r^4} - \frac{y_i y_j n_k}{r^2} - \frac{\delta_{jk}y_i y_l n_l}{r^2} - \frac{\delta_{ik}y_j y_l n_l}{r^2}\right)\bar{f}_1(\eta)\right.$$

$$\left. - \left(\frac{2\delta_{ij}y_k y_l n_l}{r^2} - \delta_{il}n_k + \frac{2y_i y_k n_j}{r^2} - \delta_{ik}n_j\right)\bar{f}_2(\eta) + \left(\frac{2y_j y_k n_i}{r^2} - \delta_{jk}n_i\right)\bar{f}_3(\eta) - \left(\frac{4y_i y_j y_k y_l n_l}{r^4}\right)\right.$$

$$\times\left\{c_1\left(\left(2+\frac{\eta^2}{4}\right)e^{-\eta^2/4}-2h_1\right)\right\}-\left(\frac{2\delta_{ij}y_k y_l n_l+2y_i y_k n_j}{r^2}\right)\{c_1(h_1-e^{-\eta^2/4})\}+\left(\frac{2y_i y_k n_j}{r^2}\right)$$

$$\times\left\{c_1\left(\left(1+\frac{\eta^2}{2}\right)e^{-\eta^2/4}-h_1\right)\right\}\Bigg]$$

$$\frac{\partial F_{ij}}{\partial \xi_k}=\frac{1}{4\pi r}\left(\frac{\beta}{\lambda+2\mu}\right)\left[\left(\frac{2y_i y_k y_l n_l}{r^3}\right)\{2h_1-e^{-\eta^2/4}\}-\left(\frac{y_k n_j}{r}+\frac{y_i n_k}{r}+\frac{\delta_{jk}y_i n_l}{r}\right)\{h_1\}\right].$$